Bioactive Materials xxx (xxxx) xxx

Contents lists available at ScienceDirect

Bioactive Materials

journal homepage: www.sciencedirect.com/journal/bioactive-materials

A low dose cell therapy system for treating osteoarthritis: *In vivo* study and *in vitro* mechanistic investigations

Bin Wang [a,b,1], Wei Liu [c,1], Jiao Jiao Li [d], Senlin Chai [a,e], Dan Xing [f], Hongsheng Yu [g], Yuanyuan Zhang [g], Wenjin Yan [a,e], Zhihong Xu [a,e], Bin Zhao [b], Yanan Du [g,**], Qing Jiang [a,e,*]

[a] *Department of Sports Medicine and Adult Reconstruction Surgery, Nanjing Drum Tower Hospital, The Affiliated Hospital of Nanjing University Medical School, Nanjing, 201180, China*
[b] *Department of Orthopaedics, Shanxi Medical University Second Affiliated Hospital, Taiyuan, 030001, China*
[c] *Beijing CytoNiche Biotechnology Co. Ltd, Beijing, 10081, China*
[d] *School of Biomedical Engineering, Faculty of Engineering and IT, University of Technology Sydney, Ultimo, NSW, 2007, Australia*
[e] *Laboratory for Bone and Joint Disease, Model Animal Research Center (MARC), Nanjing University, Nanjing, 210093, China*
[f] *Arthritis Clinic & Research Center, Peking University People's Hospital, Peking University, Beijing, 100044, China*
[g] *Department of Biomedical Engineering, School of Medicine, Tsinghua-Peking Center for Life Sciences, Tsinghua University, Beijing, 100084, China*

ARTICLE INFO

Keywords:
Osteoarthritis
Mesenchymal stem cells
Microcarriers
Tissue engineering
Transcriptome

ABSTRACT

Mesenchymal stem cells (MSCs) can be effective in alleviating the progression of osteoarthritis (OA). However, low MSC retention and survival at the injection site frequently require high doses of cells and/or repeated injections, which are not economically viable and create additional risks of complications. In this study, we produced MSC-laden microcarriers in spinner flask culture as cell delivery vehicles. These microcarriers containing a low initial dose of MSCs administered through a single injection in a rat anterior cruciate ligament (ACL) transection model of OA achieved similar reparative effects as repeated high doses of MSCs, as evaluated through imaging and histological analyses. Mechanistic investigations were conducted using a co-culture model involving human primary chondrocytes grown in monolayer, together with MSCs grown either within 3D constructs or as a monolayer. Co-culture supernatants subjected to secretome analysis showed significant decrease of inflammatory factors in the 3D group. RNA-seq of co-cultured MSCs and chondrocytes using Gene Ontology and Kyoto Encyclopedia of Genes and Genomes (KEGG) pathway analysis revealed processes relating to early chondrogenesis and increased extracellular matrix interactions in MSCs of the 3D group, as well as phenotypic maintenance in the co-cultured chondrocytes. The cell delivery platform we investigated may be effective in reducing the cell dose and injection frequency required for therapeutic applications.

1. Introduction

Osteoarthritis (OA) is a leading cause of disability worldwide, which is defined by the pathological characteristics of cartilage deterioration, aberrant bone outgrowths or osteophytes, synovitis, and subchondral bone changes [1,2]. Unfortunately, a clear mechanism for OA pathogenesis remains elusive, which creates a heavy burden for patients and their families, as well as healthcare systems due to the need for ongoing disease management [3]. Presently, the main clinical treatments for OA can be broadly classified into non-pharmacological [4], pharmacological [4], and surgical approaches [5]. However, all of these approaches are incapable of achieving tissue restoration, and each have their own limitations. Non-pharmacological treatments such as lifestyle modifications have a low risk of harm, but also have a low rate of compliance and debatable effects on long-term pain relief [6]. Pharmacological treatments such as non-steroidal anti-inflammatory drugs may provide pain relief, but are associated with an increased risk of medical complications [7]. Surgical treatment involving joint replacements,

Peer review under responsibility of KeAi Communications Co., Ltd.
* Corresponding author. Department of Sports Medicine and Adult Reconstruction Surgery, Nanjing Drum Tower Hospital, the Affiliated Hospital of Nanjing University Medical School, Nanjing, 201180, China.
** Corresponding author.
E-mail addresses: duyanan@tsinghua.edu.cn (Y. Du), qingj@nju.edu.cn (Q. Jiang).
[1] The first two authors contributed equally to this work.

https://doi.org/10.1016/j.bioactmat.2021.05.029
Received 21 March 2021; Received in revised form 28 April 2021; Accepted 17 May 2021

although effectively removing the whole joint and therefore the source of pain, has a risk of causing serious complications such as dislocation and infection [8]. There is hence a significant unmet need to develop new treatments for OA, such as those arising from tissue engineering and regenerative medicine, to provide tissue preservation or restoration and a more long-term clinical solution.

Mesenchymal stem cells (MSCs) have recently been tested in pre-clinical and clinical studies as a regenerative therapy for OA [9]. These cells have documented potential for self-renewal, directional differentiation, and immune-regulation [10–12], and also offer numerous practical benefits such as being available in the adult human and able to be extracted without donor morbidity [13–15]. However, intra-articular injection of MSCs for treating OA have not always resulted in the anticipated benefits due to a number of unoptimized parameters, such as cell number, cell retention, cell survival, and integration into the host tissue [16]. Other problems arise from the current inability to efficiently and reproducibly regulate their tissue-specific differentiation in a spatially and temporally controlled manner [17,18]. Approaches aimed at solving these problems associated with direct cell injection include loading the cells on a biomaterial matrix. This type of delivery strategy can achieve cell protection from mechanical damage during injection, as well as from the ischemic or inflammatory *in vivo* microenvironment within the lesion tissues after injection [19]. Additionally, such delivery strategies allow cells to be pre-cultured or expanded within the biomaterial prior to injection, which removes the need to detach cells from their adhesion surface directly before transplantation, a process that could otherwise be detrimental to cell survival and result in poor clinical outcomes [20].

The majority of biomaterial matrices used for intra-articular cell delivery are in the form of hydrogels due to their injectability. However, hydrogels are inefficient in promoting extracellular matrix (ECM) accumulation or cell-cell interactions for the encapsulated cells [21,22]. Additionally, it has been reported that instead of a single dose, periodic injections of MSCs should be used for OA treatment to maintain a viable source of cells within the joint, which was shown to have improved effects at slowing OA progression in both animal models and human knee OA [23–25]. A higher dose of MSCs has also been reported to achieve greater benefits than a low dose [26]. However, implementing high injection frequency and/or cell dose in OA treatment is problematic, due to issues of increasing the local complication rate [27], and wasting cell resources or risking the over-expansion of cells [28], respectively. An ideal biomaterial platform for cell delivery in OA treatment should therefore be injectable, while at the same time presenting the cells with a three dimensional (3D) microenvironment that enhances native cell-cell interactions and ECM deposition, to maximize cell functionality and therefore reduce the injection frequency and cell dose required for therapeutic effects.

Our group has previously developed 3D gelatin microcarriers that can be used as cell delivery vehicles. When loaded with cells, these microcarriers form microniches that allow local accumulation of ECM and cell-cell interactions [29]. When packed into a geometrically confined 3D environment, the microniches may further self-assemble into functional 3D constructs [30]. We have shown that these injectable 3D microniches can increase the efficiency of cell therapy, whereby a low cell dose delivered within microniches can achieve similar effects as a high cell dose delivered directly in rat models of knee OA [31] and critical limb ischemia [28]. However, we have not optimized the methods for the efficient production of cell-laden microniches that would be suitable for scale-up applications, or the functionality of the microniches to ideally substitute for both high-dose cell injection and repeated injections. Furthermore, we have not performed detailed investigations on the interactions between cell-laden microniches and resident cells to understand the precise mechanisms driving the observed therapeutic effects in a pathological joint environment.

The scalable and controllable expansion of MSCs is a primary hurdle that needs to be overcome when developing cell therapy products aimed at practical applications [32]. For cells loaded within micro-scaffolds, stirred-tank bioreactors are one of the most cost-effective types of bioprocessing systems that can efficiently increase nutrient supply [19] compared to conventional monolayer cultures [33]. For instance, cells pre-cultured within scaffolds under the dynamic culture conditions provided by a spinner flask bioreactor have shown increased rates of proliferation and ECM synthesis [34]. MSCs combined with polymeric scaffolds [35,36] or microspheres [37] and cultured in spinner flasks have also shown improved formation of chondrogenic constructs compared to those cultured under static conditions. In this study, we have tested for the first time a single injection of microniches seeded with a low MSC dose and pre-cultured in spinner flasks, compared with repeated high-dose injections of MSCs for their therapeutic effects in an *in vivo* rat model of knee OA.

Several studies have introduced co-culture systems between MSCs and chondrocytes to investigate the mechanisms underlying intercellular communication and trophic effects, mimicking the *in vivo* interactions between injected exogenous MSCs and resident chondrocytes in physiological and pathological joint environments [38–40]. It is generally believed that molecular factors passed between the two cell types in a co-culture system are responsible for changes in their expression profiles, which may sometimes result in mutually beneficial effects [41]. In this study, to understand the mechanisms underlying the observed effects of MSC-laden microniches after being injected into the *in vivo* OA model, we for the first time established an *in vitro* co-culture system consisting of OA chondrocytes cultured in monolayer and primed in an inflammatory environment (through interleukin-1β (IL-1β) stimulation), together with MSCs growing in monolayer or within microcarriers. We characterized the secretome and transcriptome of MSCs and chondrocytes in this co-culture system.

Our study aimed to use *in vivo* (rat anterior cruciate ligament (ACL) transection OA model) and *in vitro* (MSC and chondrocyte co-culture) systems to simulate the chronic OA environment, for investigating 1) the therapeutic effects of a single injection of cell-laden microniches with a low dose of MSCs, and 2) the mechanisms by which MSCs cultured in microcarriers produce a beneficial response compared to free MSCs. We showed that a low dose of MSCs administered through microniches produced similar therapeutic effects in a rat model of OA as repeated injections of high-dose free MSCs, and that MSCs cultured in microcarriers may better promote the activation of pathways leading to early chondrogenesis and maintenance of the chondrocyte phenotype.

2. Materials and methods

2.1. Preparation and characterization of gelatin microgels

Gelatin microcarriers (“3D FloTrix” supplied by Beijing CytoNiche Biotech Ltd) were fabricated as previously described to give spherical micro-scaffolds with uniform diameter, degradation time, and water absorption [19,29]. The microcarriers were sputter coated with gold for 90 s and imaged using scanning electron microscopy (SEM; FEI Quanta 200). The pore size distribution of scaffolds was measured using ImageJ by sampling 8 regions each in 12 different SEM images.

2.2. Preparation and characterization of MSC-laden microniches

2.2.1. Preparation of MSC-laden microniches using spinner flask culture

Microniches were prepared by loading MSCs into gelatin microcarriers. Five tablets of compressed gelatin microcarriers (3D FloTrix) were placed in a sterile 125 mL spinner flask (SF125, CytoNiche Biotech, China) with 10 mL cell culture medium (M001, Viral Therapy Technologies, China) through the side arm and fully dispersed by gentle agitation. A 1 mL cell suspension containing 5×10^6 human umbilical cord MSCs (non-commercial; provided by Clinical Stem Cell Center, The Affiliated Drum Tower Hospital of Nanjing University Medical School) at passage 3 were then added, and culture medium was immediately

topped up to a final volume of 40 mL. The spinner flasks were placed on a miniSPIN system (M1, CytoNiche Biotech, China) set up inside a cell culture incubator, and rotated at 60 rpm. MSC-laden microniches were cultured in spinner flasks at 37 °C and 5% CO_2 for up to 14 days, with 20 mL of fresh culture medium replaced from the flask every 3 days.

2.2.2. Live/dead staining of MSCs in microniches

After 1, 3, 7, and 14 days of culture in spinner flasks, live/dead staining with Calcein AM and Propidium iodide (PI) (Wako, Japan) of MSCs within microniches was performed at 37 °C for 15 min according to the manufacturer's instructions. Cells on microcarriers were enumerated by dissolving microcarriers with 3D FloTrix Digest (CNR001-500, CytoNiche Biotech, China) reagent at a ratio of 0.15 mL mg^{-1} microcarriers for 30 min at 37 °C. Cell numbers were counted with an automatic cell counter (Countstar Biotech, ALIT Life Science, China), and viability was evaluated with Trypan Blue exclusion assay [34].

2.2.3. Quantitative RT-PCR of MSCs in microniches

Total RNA of MSCs in microniches was isolated using the TRIzol reagent (Invitrogen) according to the manufacturer's instructions. For each sample, reverse transcription was performed using the ReverTra Ace Qrna RT Master Mix with gDNA Remover (TOYOBO). Quantitative RT-PCR (qRT-PCR) was performed using the CFX96 Real-Time System (Bio-Rad, USA). Samples were denatured for 30 s at 95 °C, and then amplified for 40 cycles as follows: denaturation at 95 °C for 5 s, annealing at 55 °C for 10 s, and extension at 72 °C for 15 s. The Ct values of the products were normalized to glyceraldehyde-3-phosphate dehydrogenase (GAPDH) as an internal control, and the expression levels of the genes of interest were calculated using the $2^{-\Delta\Delta CT}$ method. Primer details are shown in Table 1.

2.2.4. Flow cytometry of MSCs in microniches

MSCs digested from microniches were stained with antibodies against the MSC markers CD73, CD90 and CD105, and the negative markers CD34 and CD45. Unstained MSCs were used as negative control. The cells were analyzed by flow cytometry (BD LSRFortessa, US).

2.2.5. In vivo cell retention of MSCs in microniches

Cell deliverability and long-term retention of MSCs within microniches was tested using an *in vivo* mouse model, using methods adapted from our previous study [28]. A firefly Akalumine Hydrochloride (AkaLuc-HCL) expression vector was constructed on plasmid pLVX-IREs-IsGreen (Clontech, USA). Lentiviruses were packaged in 293T cells with a three-plasmid system, comprising pMD2.G, psPAX and pLVX vectors (CytoNiche Biotech, China). MSCs were then infected with AkaLuc-HCL lentiviruses, with a positive rate of greater than 90%. AkaLuc-transduced MSCs (luc^{+}MSCs) were injected subcutaneously around both knee joints in six male BALB/c mice (200–250g, 4–6 weeks), either as 1×10^6 cells loaded within microniches or as free cells in the contralateral limb. High-sensitivity bioluminescence imaging was performed to track the retention of cells on days 1, 7, 14, and 21 after injection using a Xenogen IVIS Lumina II imaging system (Caliper Life Science, USA). The luminescence signal is presented as photons per second per square centimeter per steradian (photons/s/cm^2/sr).

Table 1
Details of primer.

Primers	Primer sequence
SOX2	Forward: ACACCAATCCCATCCACACT
	Reverse: GCAAACTTCCTGCAAAGCTC
OCT4	Forward: AGCGAACCAGTATCGAGAAC
	Reverse: GCCTCAAAATCCTCTCGTTG
NANOG	Forward: TGAACCTCAGCTACAAACAG
	Reverse: CTGGATGTTCTGGGTCTGGT
P16	Forward: ATATGCCTTCCCCCACTACC
	Reverse: CCCCTGAGCTTCCCTAGTTC
P21	Forward: CCCAGTTCATTGCACTTTGATTAGC
	Reverse: ACAGTCTAGGTGGAGAAACGGGAAC
P53	Forward: CCCATCCTTACCATCATCACG
	Reverse: TGCTGGTGGGCAGTGCTCTCT
SOX9	Forward: AGCGAACGCACATCAAGAC
	Reverse: CTGTAGGCGATCTGTTGGGG
Col2A1	Forward: CCAGATGACCTTCCTACGCC
	Reverse: TTCAGGGCAGTGTACGTGAAC
AGG	Forward: GTGCCTATCAGGACAAGGTCT
	Reverse: GATGCCTTTCACCACGACTTC
GAPDH	Forward: TGCACCACCAACTGCTTAGC
	Reverse: GGCATGGACTGTGGTCATGAG

2.3. Rat ACL transection model of knee OA

2.3.1. Surgical procedures

The animal experiments were conducted in accordance with guidelines of the Institutional Animal Care and Use Committees (IACUC), and approved by the Ethics Committee of Shanxi Medical University (No. 2018LL036). A total of 40 female Sprague Dawley rats (mean weight 200g) were randomly divided into 5 groups. A 1.5 cm midline skin incision was made over the knee joint by using a #12 blade scalpel. Superficial fascia tissues and capsule were then exposed using a medial parapatellar approach. With the knee in full extension, the patella was retracted laterally, then the joint was brought back into full flexion. The ACL was visualized and transected at its mid-point using a surgical blade scalpel. The capsule and surgical wound were closed using 4-0 Prolene sutures. The 5 groups were treated at 6 weeks post-surgery: sham, hyaluronic acid (HA), lowMSCs/microniches, highMSCs and ctrl. Sham: animals with surgery only but no treatment. HA: hyaluronic acid (Shandong Boshlun Freida Pharmaceutical Co., Ltd) injections of 200 μL per knee per week for 4 weeks. LowMSCs/microniches: microniches containing 1×10^5 MSCs were cultured in spinner flasks for 2 days prior to injection, which were collected and centrifuged just before the time of injection, and injected in 200 μL PBS per knee as a single injection. HighMSCs: 1×10^6 free MSCs injected in 200 μL PBS per knee per week for 4 weeks. Ctrl: animals without surgery.

2.3.2. MRI analysis

All rats undergoing magnetic resonance imaging (MRI) were anesthetized with a halothane-oxygen mixture in a closed box. The rat was placed in a supine position with the rear legs stretched straight. A respiratory sensor was used for monitoring respiratory conditions and delivering the halothane-oxygen mixture. A separate quadrature surface coil (BioSpec70/20USR, Bruke, Germany) for signal detection was placed above both knee joints to reach maximum signal intensity. After image acquisition was completed, the data were transferred to a standalone computer for final analysis.

2.3.3. X-ray analysis

Rats were sacrificed at 12 weeks after ACL transection. Explanted knee joints were fixed with 4% paraformaldehyde and evaluated using a small-animal X-ray apparatus (Faxitron UltraFocus, Arizona, USA). X-ray images were taken from knee joints in the anteroposterior position. The exposure time and kV settings were set at "full AUTO".

2.3.4. Micro-CT analysis

Explanted knee joints were scanned using μ-CT (SC5814, Scanco, Switzerland), using the following parameters: 70 kV (voltage), 200 μA (current), 30 μm (resolution), 300 ms (exposure time). After image reconstruction, the region of interest (ROI) of knees was assigned. The 3D reconstructed images were evaluated and visualized using Inveon Research Workplace (Siemens) software. A semiquantitative method using the degree of osteophytes and joint destruction was introduced to grade the degree of OA changes [31].

2.3.5. Histological analysis

Explanted knee joints were fixed in 10% formalin for a minimum of

72 h prior to decalcification with ethylenediaminetetraacetic acid (EDTA) for 3 weeks. After serial dehydration, samples were embedded in paraffin. Knees were cut longitudinally (4 μm) along the coronal face. Safranin O and hematoxylin and eosin (H&E) staining were applied to detect cartilage degeneration using light microscopy. The Osteoarthritis Research Society International (OARSI) [42] and Mankin's score [43] were used to grade cartilage quality.

2.4. Co-culture model of OA with human chondrocytes and MSCs

2.4.1. Human chondrocyte isolation and culture

Primary human chondrocytes were isolated from the femoral condyles of patients undergoing total knee arthroplasty (TKA) due to knee OA. The inclusion criteria for patient selection were: 1) end-stage primary knee OA and undergoing TKA. The exclusion criteria were: 1) rheumatoid arthritis, 2) post-traumatic OA, and 3) having other conditions contributing to the need for TKA, such as hemophilia or ankylosing spondylitis. Patient characteristics are presented in Table S1. All procedures were conducted with the patients' written consent and approved by the Nanjing Tower Drum Hospital Ethics Committee (2020-156-01). Briefly, isolated cartilage samples were cut into small pieces and washed with PBS before digestion with 0.1% collagenase D-containing DMEM media (Gibco) for 8 h. The cells were then dispensed over a 100 μm cell strainer (BD, Falcon) positioned over a 15 ml conical tube. Cells were centrifuged at 1500 rpm for 5 min, and the supernatants containing collagenase D were removed. The resulting primary chondrocytes were cultured in 6-well plates in Dulbecco's modified eagle medium (DMEM, Gibco) supplemented with 15% fetal calf serum (FBS; Invitrogen), 1% glutamine, 100 units/mL penicillin, 100 units/mL streptomycin, and 0.05 mg/mL ascorbic acid. Cultures were maintained at 37 °C and 5% CO_2 for 7 days until the cells reached 70–80% confluence, which was designated as passage 0.

2.4.2. Co-culture of chondrocytes and MSCs using transwells

Co-cultures using patient unmatched cells were set up using a transwell system, in which the two cell types not physically separated and allowed to interact only through diffusible factors. Chondrocytes (1×10^5 cells/cm^2) were grown in monolayer on 6-well plates (Corning/Costar 3516, USA), while MSCs (1×10^6 cells/cm^2) were grown on 6-well hanging inserts (Millicell, pore size 0.4 μm, Germany) under liquid-covered conditions, either as a monolayer (2D group) or within microniches (3D group). MSC-laden microniches in the 3D group were added to the co-culture system 2 h after the MSCs were seeded within microcarriers to allow cell adhesion [28,30]. The co-cultures were cultivated at 37 °C and 5% CO_2 for 7 days, in DMEM medium containing 10% (v/v) FBS and 1% (v/v) P/S. All co-cultures were stimulated with IL-1β (10 ng/ml) for 48 h before conducting qRT-PCR and Western blot analyses. Previous literature has suggested that 24 h is a suitable period for IL-1β stimulation of chondrocytes in monolayer [44]. Based on our preliminary investigations for IL-1β stimulation of monolayer chondrocytes in our co-culture system for 24, 48 and 72 h (data not shown), which involved an increased volume of culture medium and an additional cell type (MSCs), 48 h was the optimal stimulation time based on chondrocyte phenotype maintenance.

2.4.3. qRT-PCR analysis of chondrocytes and MSCs

Gene expression analysis of co-cultured chondrocytes and MSCs was conducted using qRT-PCR according to procedures described in Section 2.2.3.

2.4.4. Western blot analysis of chondrocytes and MSCs

Protein expression levels of type II collagen (SC-52658, Santa Cruz, USA), SOX9 (ab3697, Abcam, USA), and GAPDH in co-cultured chondrocytes and MSCs were measured using Western blot. Cytosolic proteins were directly extracted with radio immune precipitation assay (RIPA) lysis buffer combined with a cocktail of protease and phosphatase inhibitors. The protein concentration was calculated using the BCA Protein Assay Kit (Promega). Western blot was performed using a kit (Beyotime, Biotechnology) according to the manufacturer's instructions, and ECL reagent was used to generate chemiluminescent signals.

2.4.5. Secretome analysis of co-culture supernatants

Cells in the 2D and 3D co-culture groups were washed twice in PBS and then cultured under starvation in non-supplemented F12 medium (Gibco, USA) for 24 h. The co-culture supernatants were collected and analyzed for 40 secreted proteins using the Proteome Profiler Human Inflammation Array Q3 (QAH–INF–3-1, RayBiotech Systems) according to the manufacturer's instructions. Briefly, slides were held by the edges to make a small marking along the top edge. The array area was blocked, washed and incubated overnight at 4 °C on a rocking platform with 0.1 mL of standard cytokines or culture supernatant (at 10 × concentration). Each well was then washed and incubated with Biotinylated antibody cocktail for 2 h at room temperature on a rocking platform. The slide was incubated with Cy3 Equivalent Dye-Streptavidin and imaged using the InnoScan 300 Microarray Scanner (Innopsys, France). After correcting for background intensity and normalizing to the slide's positive control, expression levels of cytokines were detected by microarray analysis and drawn as a heat map.

2.4.6. RNA-seq analysis of chondrocytes and MSCs

The procedure for RNA-seq was modified based on previously published methods [45]. Briefly, total RNA was extracted from both chondrocytes and MSCs in the 2D and 3D groups using the TRIzol reagent (Invitrogen). RNA purity was checked using the NanoPhotometer spectrophotometer (IMPLEN, USA), and RNA integrity was assessed using the RNA Nano 6000 Assay Kit of the Bioanalyzer 2100 system (Agilent Technologies, USA). The sequencing library was constructed using the NEBNext UltraTM RNA library Prep Kit for Illumina (NEB, USA) according to the manufacturer's instructions. Index of the reference genome was built using Hisat2 v2.0.5. Differential expression analysis between groups (two biological replicates per condition) was performed using the DESeq2 R package. All statistical analyses were conducted using R statistical programming language. Genes with an adjusted p-value of <0.05 found by DESeq2 were assigned as differentially expressed. Differentially expressed genes (DEGs) were defined as having a fold change ≥ 2 and p-value ≤ 0.05. Heatmaps were generated using the heatmap package. Gene ontology (GO) enrichment analysis and KEGG pathway analysis were performed using clusterProfiler R package. For each group, 3 duplicates were collected for RNA-seq analysis.

2.5. Statistical analysis

Statistical analysis was performed using GraphPad Prism. All data are presented as mean ± standard deviation (SD). Student's t-test was used when comparing two groups of data, and one-way analysis of variance (ANOVA) followed by Tukey's post hoc test was used when comparing between three or more groups. Values of $p < 0.05$ were considered to be statistically significant. All experiments were performed using at least three independent samples.

3. Results

3.1. Study design

A schematic overview of the study design is shown in Fig. 1. Gelatin microcarriers were fabricated with uniform diameter (Fig. 1A and B). MSCs were seeded in spinner flasks and cultured together with microcarriers for 2 days to form MSC-laden microniches (Fig. 1C and D). These microniches were then used for injection in a rat ACL transection model of knee OA (Fig. 1E and F). A co-culture system was used to investigate

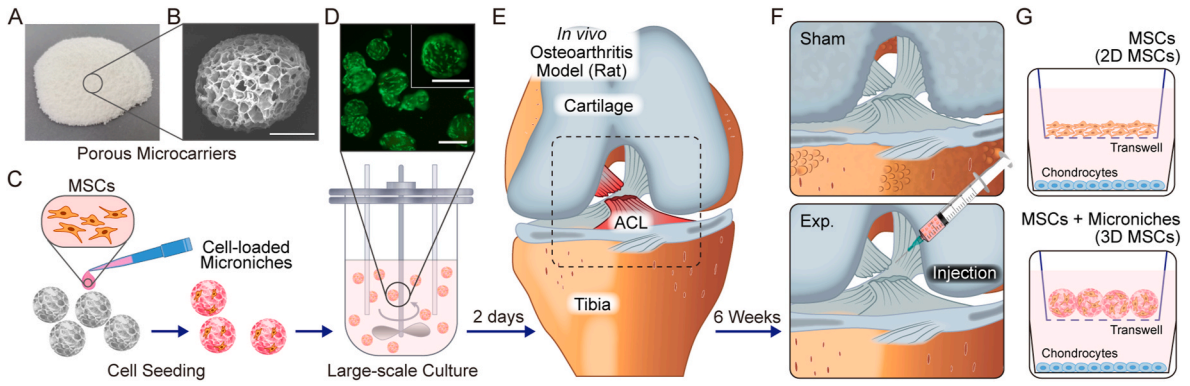

Fig. 1. Schematic illustration of the overall study design. (A, B) Gelatin microcarriers with interconnected porosity were fabricated with unified diameter, scale bar = 100 μm. (C, D) MSCs were seeded in microcarriers and cultured in a customized spinner flask to form MSC-laden microniches, scale bar = 100 μm. (E, F) After *in vitro* culture for 2 days, the MSC-laden microniches were injected as treatment in a rat ACL transection model of knee OA. Sham: animals with surgery only but no treatment. Experiment: treatment by injection with MSC-laden microniches. (G) A transwell co-culture system was used for mechanistic investigations of the interactions between MSCs and chondrocytes in an OA environment.

the mechanism of interactions between MSCs and chondrocytes in an OA environment (Fig. 1G).

3.2. Characterization of MSC-laden microniches produced using spinner flask culture

The gelatin microcarriers were supplied as compressed tablets which

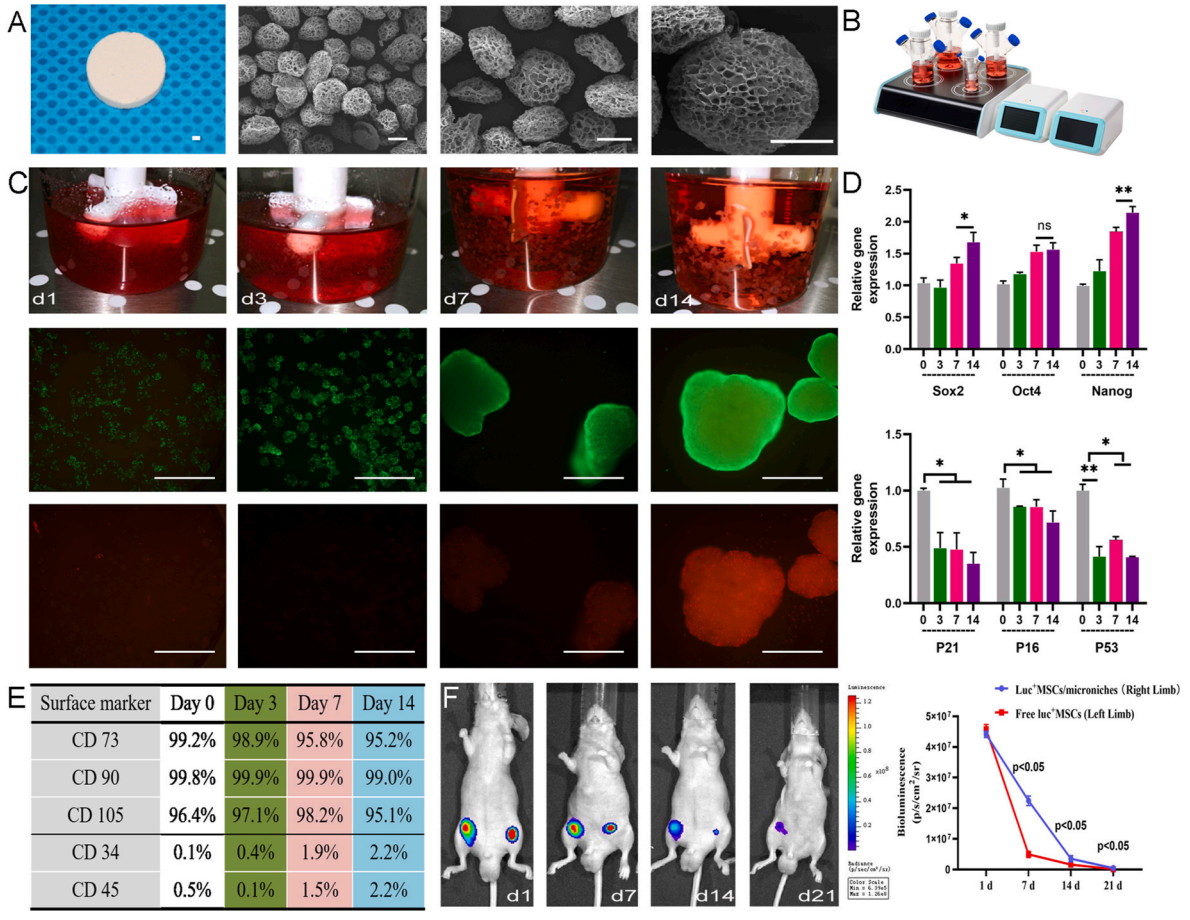

Surface marker	Day 0	Day 3	Day 7	Day 14
CD 73	99.2%	98.9%	95.8%	95.2%
CD 90	99.8%	99.9%	99.9%	99.0%
CD 105	96.4%	97.1%	98.2%	95.1%
CD 34	0.1%	0.4%	1.9%	2.2%
CD 45	0.5%	0.1%	1.5%	2.2%

Fig. 2. Characterization of MSC-laden microniches produced using spinner flask culture. (A) Photograph of the compressed microcarrier tablet, and SEM images of the dispersed microcarriers upon contact with an aqueous medium. Scale bar (left to right) = 100 μm. (B) Spinner flask culture system with controller, magnetic stirrer and spinner flasks. (C) Fluorescent images of live/dead staining of MSCs on days 1, 3, 7, and 14 of culture, scale bar = 500 μm. (D) Relative gene expression of stemness-related markers (SOX2, OCT4, NANOG) and senescence-related markers (P21, P16, P53) in MSC-laden microniches over 14 days of culture (n = 3). (E) Flow cytometry analysis of surface biomarker expression over 14 days (n = 1, corresponding to a pool of 3 microniches). (F) Bioluminescence imaging for tracking *in vivo* cell retention for injected MSC-laden microniches, showing measurements of average radiance in standardized regions of interest from the hindlimb of mice on days 1, 7, 14 and 21. Luminescence signal is presented as photons per second per square centimeter per steradian (n = 3).

dispersed into individual microcarriers upon contact with an aqueous medium. The microcarriers exhibited a uniform diameter of 200 ± 7.35 μm, together with high porosity (>80%) and interconnected macroporous structure, as shown in SEM images (Fig. 2A). The pore diameter distribution analyzed using ImageJ was 17.78 ± 6.3 μm. The microcarriers were cultured together with MSCs in spinner flasks to allow the formation of MSC-laden microniches (Fig. 2B).

3.2.1. Live/dead staining of MSCs in microniches

Live/dead staining with Calcein AM/PI showed that the majority of MSCs growing in microniches during spinner flask culture over 14 days remained viable (Fig. 2C). The MSCs deposited ECM within the microniches at days 2–3, and then formed larger constructs at the later time points. The number of MSCs in microniches showed significant increases at day 2–3 (Fig. S1), but not at day 7 or 14 (data not shown). To ensure cell quantity and quality for *in vivo* testing, we selected 2 days as the preculture period for MSC-laden microniches before they were used for injection into animals.

3.2.2. Quantitative RT-PCR of MSCs in microniches

MSCs in microniches were evaluated for stemness and senescence related gene markers by qRT-PCR (Fig. 2D). The stemness-related markers SOX2, OCT4 and NANOG showed higher expression at 7 and 14 days compared to earlier time points. In contrast, the senescence-related markers P21, P16 and P53 showed significant downregulation after 3 days, matching the time frame at which self-assembly of microniches commenced as shown by the live/dead staining images. The gene expression results collectively suggested that the MSCs could maintain their stemness and suppression of senescence while the microniches were cultured for 7–14 days in spinner flasks. It is expected that similar effects would persist *in vivo* for at least 1–2 weeks after MSC-laden microniches pre-cultured for 2 days are injected into animals.

3.2.3. Flow cytometry of MSCs in microniches

Flow cytometry results demonstrated that MSCs in microniches retained their immunophenotype during spinner flask culture, with high expression of the MSC markers CD73, CD90 and CD105, as well as low expression of the negative markers CD34 and CD45 (Fig. 2E). The proportion of surface marker expression did not show significant changes over the 14 days culture period.

3.2.4. In vivo cell retention of MSCs in microniches

Luciferase-transduced MSCs (luc^{+}MSCs) were subcutaneously injected into the thighs of mice as free MSCs (left) or loaded within microniches (right). The microniches luc^{+}MSCs showed more constant bioluminescence between 7 and 21 days, suggesting stable cell retention

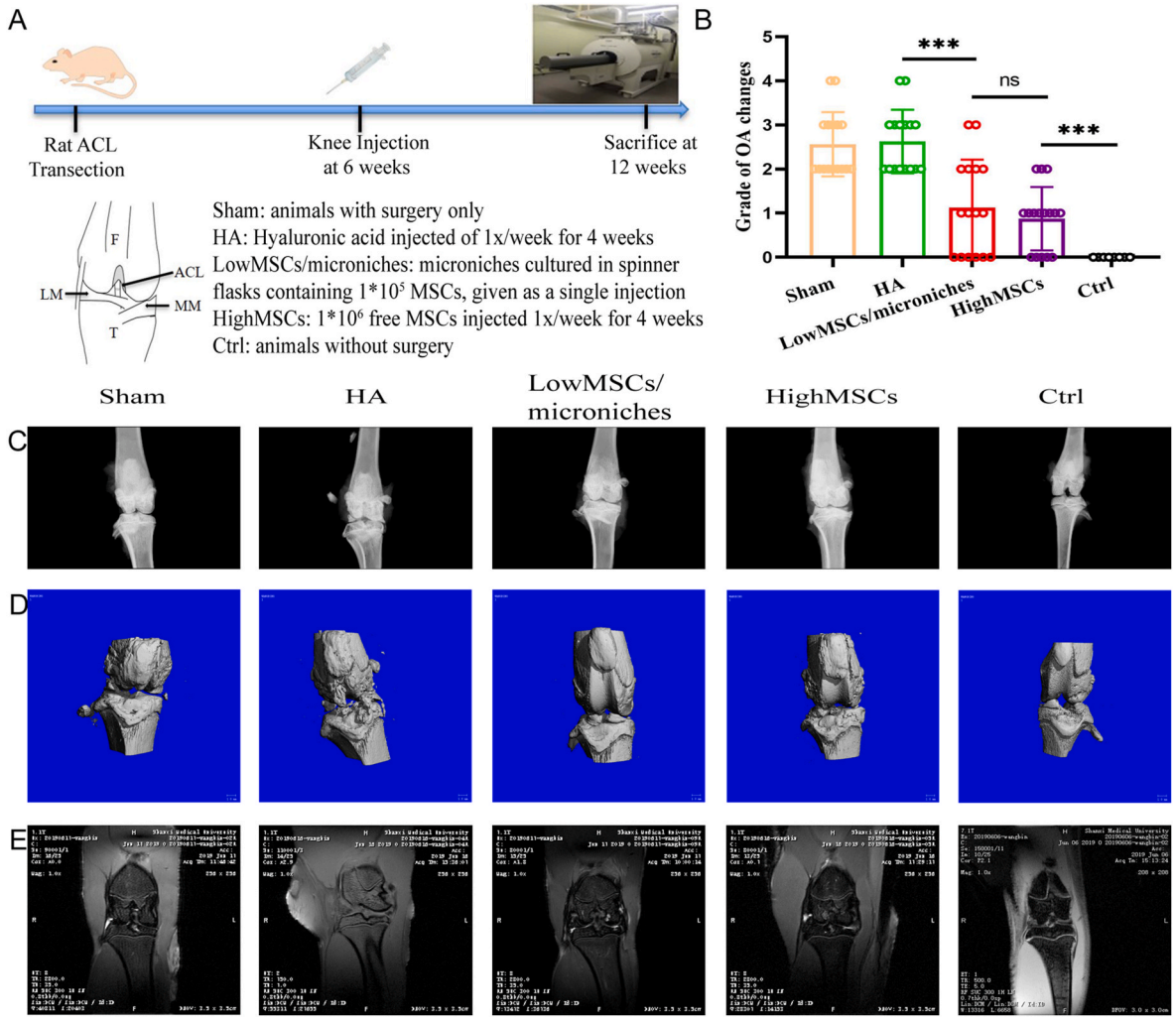

Fig. 3. Imaging analyses of MSC-laden microniches in a rat ACL transection model of knee OA. (A) Schematic illustration of the overall animal study design. Six weeks after ACL transection, rat knees with OA were divided into sham, HA, lowMSCs/microniches, highMSCs and control groups. (B) The grade of OA changes based on μ-CT analysis in all groups at 6 weeks after treatment. Representative images from (C) X-ray, (D) μ-CT, and (E) MRI analysis in all groups at 6 weeks after treatment.

and sustained viability within microniches at the injection site over the 21 day period (Fig. 2F). In contrast, the free luc $^{+}$ MSCs underwent greater dispersion after 7 days with dramatic cell loss and deteriorated bioluminescence. The imaging data was quantified and presented as a measurement of the average radiance in standardized regions of interest on the thigh. The improved *in vivo* MSC retention and survival within microniches might enable better delivery of their therapeutic functions after injection.

3.3. Effects of MSC-laden microniches in a rat ACL transection model of knee OA

The rats developed knee OA at 6 weeks after ACL transection. All animals tolerated the bilateral transection model, and could bear the load of their own weight on the day after surgery. Rat knees were injected with HA (four times, one week apart), large dose of free MSCs (four times, one week apart), or low dose of MSCs in microniches (once) at 6 weeks after ACL transection, and the animals were sacrificed at 12 weeks (Fig. 3A).

3.3.1. X-ray, μ-CT and MRI analyses

X-ray images showed that the LowMSCs/microniches and HighMSCs groups had better treatment effects compared to the HA and sham groups, with less osteophyte formation and joint narrowing (Fig. 3C). These observations were confirmed by the μ-CT reconstructed images (Fig. 3B, D). MRI images showed that the LowMSCs/microniches and HighMSCs groups had less knee effusion compared to the HA and sham groups, suggesting less severe progression of OA (Fig. 3E).

3.3.2. Histological analysis

H&E and Safranin O (Fig. 4A) staining were performed on coronal sections of explanted knees. The histological images were scored using the OARSI (Fig. 4B) and Mankin's (Fig. 4C) grading systems. Although all groups had significantly higher scores compared to the control, the LowMSCs/microniches and HighMSCs groups showed significantly lower scores compared to the HA and sham groups, with values that were more similar to control (normal) knees. Scores for the LowMSCs/microniches and HighMSCs groups also had similar values. The histological results indicated that a low dose of MSCs in microniches had similar effects as repeated high doses of free MSCs in helping to preserve and restore cartilage integrity in an *in vivo* model of induced knee OA.

3.4. Human chondrocyte and MSC interactions in a co-culture model of OA

A transwell system was used to examine the influence of MSC culture in microniches (3D group) compared to monolayer (2D group) when co-cultured with chondrocytes in monolayer on their secretome and transcriptome (Fig. 5A).

3.4.1. qRT-PCR and Western blot analyses of chondrocytes and MSCs

Gene and protein expression analyses both indicated that the chondrocytes co-cultured with MSCs in microniches (3D group) had higher expression of chondrogenesis-related markers, namely collagen type II and SOX9, compared to those co-cultured with MSCs in monolayer (2D group) (Fig. 5B). In the same co-culture system, MSCs in the 3D group had higher expression of chondrogenesis-related gene and protein markers compared to those in the 2D group.

3.4.2. Secretome analysis of co-culture supernatants

The secretome of co-culture supernatants was compared between the 2D and 3D groups at 7 days using their cytokine profile, with DMEM/F-12 (Gibco, USA) used as a control. There were 4 of 40 cytokines that exhibited significantly different staining intensity between groups: IL-1β, IL-1α, GM-CSF and IL-6R (Fig. 5C). Among these, granulocyte macrophage–colony stimulating factor (GM-CSF) has important roles in cartilage repair, and it significant increase in the 3D group together with decrease in IL-6R suggest anti-inflammatory and reparative effects of 3D MSC culture in microniches. Gene Ontology (GO) enrichment analysis showed prominent regulation of pathways relating to cytokine production and cytokine receptor binding in the 3D group, which possibly contribute to the anti-inflammatory effects observed in this group. Similarly, KEGG pathway analysis showed significant induction of "cytokine-cytokine receptor interaction" in the 3D group (Fig. 5D, S2).

3.4.3. RNA-seq analysis of chondrocytes and MSCs

Whole transcriptome RNA sequencing was performed on MSCs and chondrocytes in the 2D and 3D groups. Heat maps were drawn to compare differentially expressed genes (DEGs) in the co-cultured MSCs and chondrocytes, relative to a monolayer control (Fig. 6A). MSCs in the 3D group had 6371 DEGs, including 3005 upregulated and 3366 downregulated genes, while MSCs in the 2D group had 4992 DEGs, including 2270 upregulated and 2722 downregulated genes. Chondrocytes in the 3D group had 5891 DEGs, including 2671 upregulated and 3130 downregulated genes, while chondrocytes in the 2D group had 6461 DEGs, including 3084 upregulated and 3377 downregulated genes

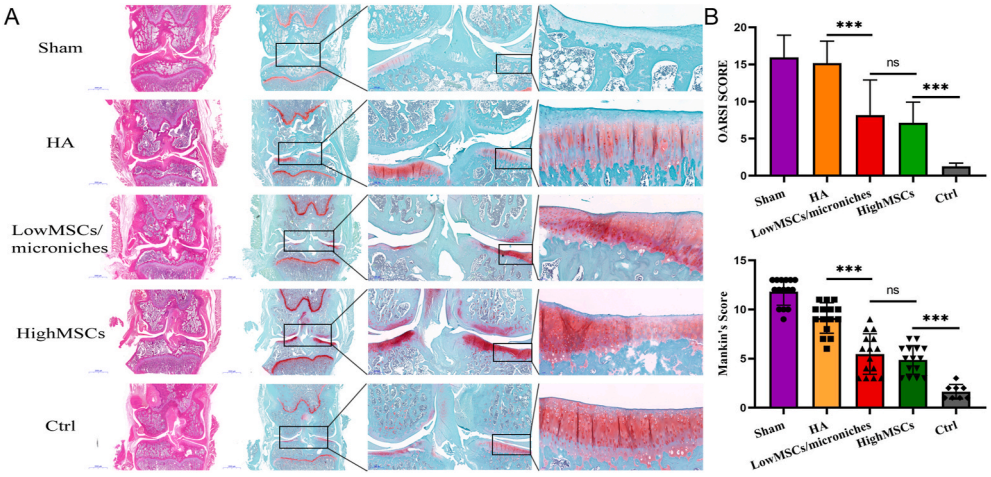

Fig. 4. Histological analysis of MSC-laden microniches in a rat ACL transection model of knee OA. (A) Light microscopy images of articular cartilage on coronal sections from explanted knees in all groups, stained by H&E and Safranin O. (B) OARSI and (C) Mankin's histological assessment scores for all groups at 6 weeks after treatment.

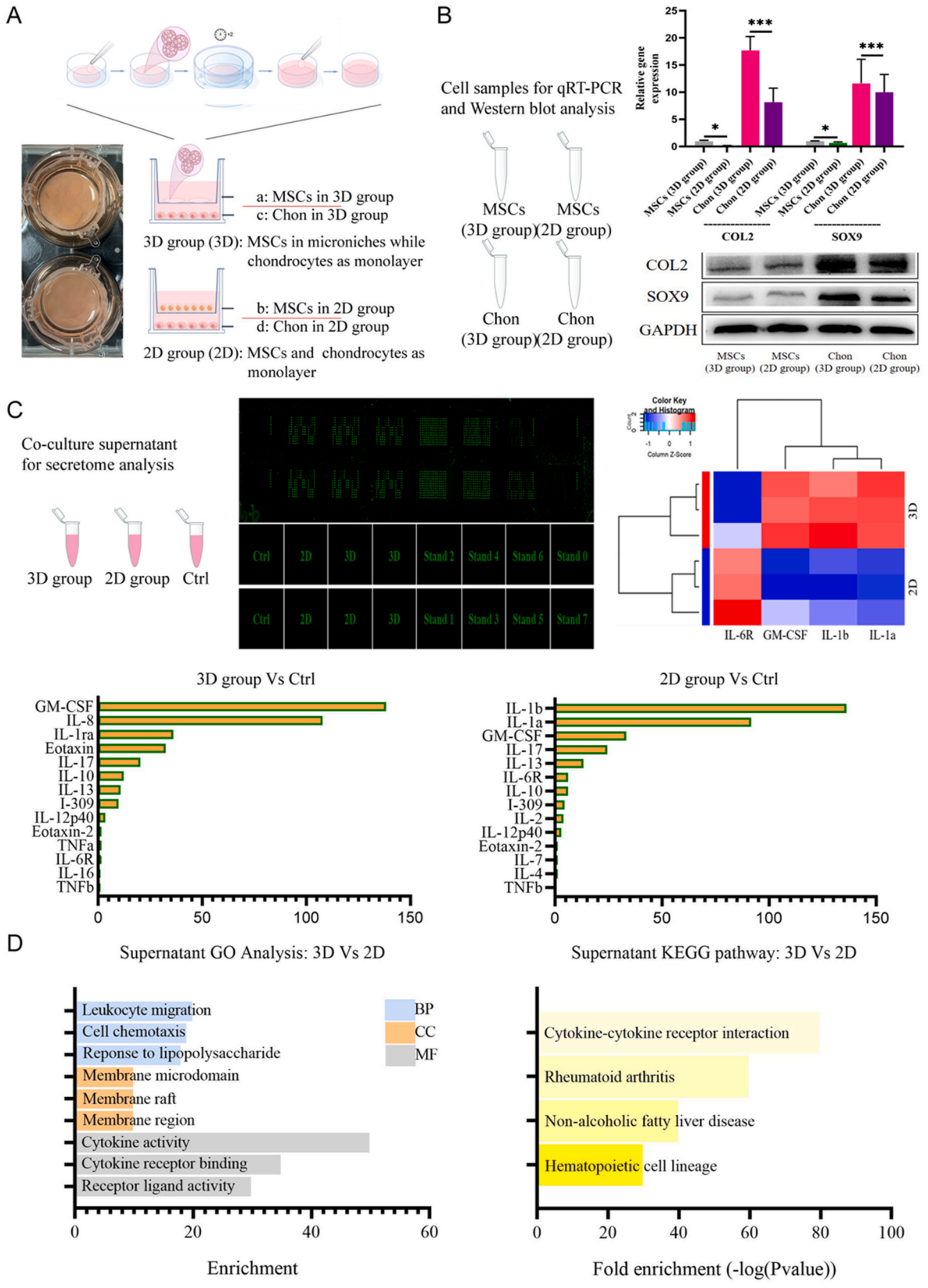

Fig. 5. Secretome analysis of chondrocyte and MSC co-culture supernatants. (A) Schematic illustration of the transwell system for co-culturing human chondrocytes and MSCs. The 3D group consisted of MSCs in microniches while the 2D group consisted of MSCs in monolayer, with both groups having chondrocytes in monolayer. (B) Relative gene and protein expression of chondrogenesis-related markers (COL2, SOX9) in chondrocytes and MSCs of the 3D and 2D groups (n = 3). (C) Secretome analysis of culture supernatants conducted by comparing cytokine profiles between groups. A heat map of 4 incubated cytokines that exhibited significantly different staining intensity among groups is presented, along with relative expression levels of 13 inflammatory cytokines. (D) GO enrichment analysis and KEGG pathway analysis of co-culture supernatants compared between the 3D and 2D groups. BP: Biological Process; CC: Cellular Component; MF: Molecular Function.

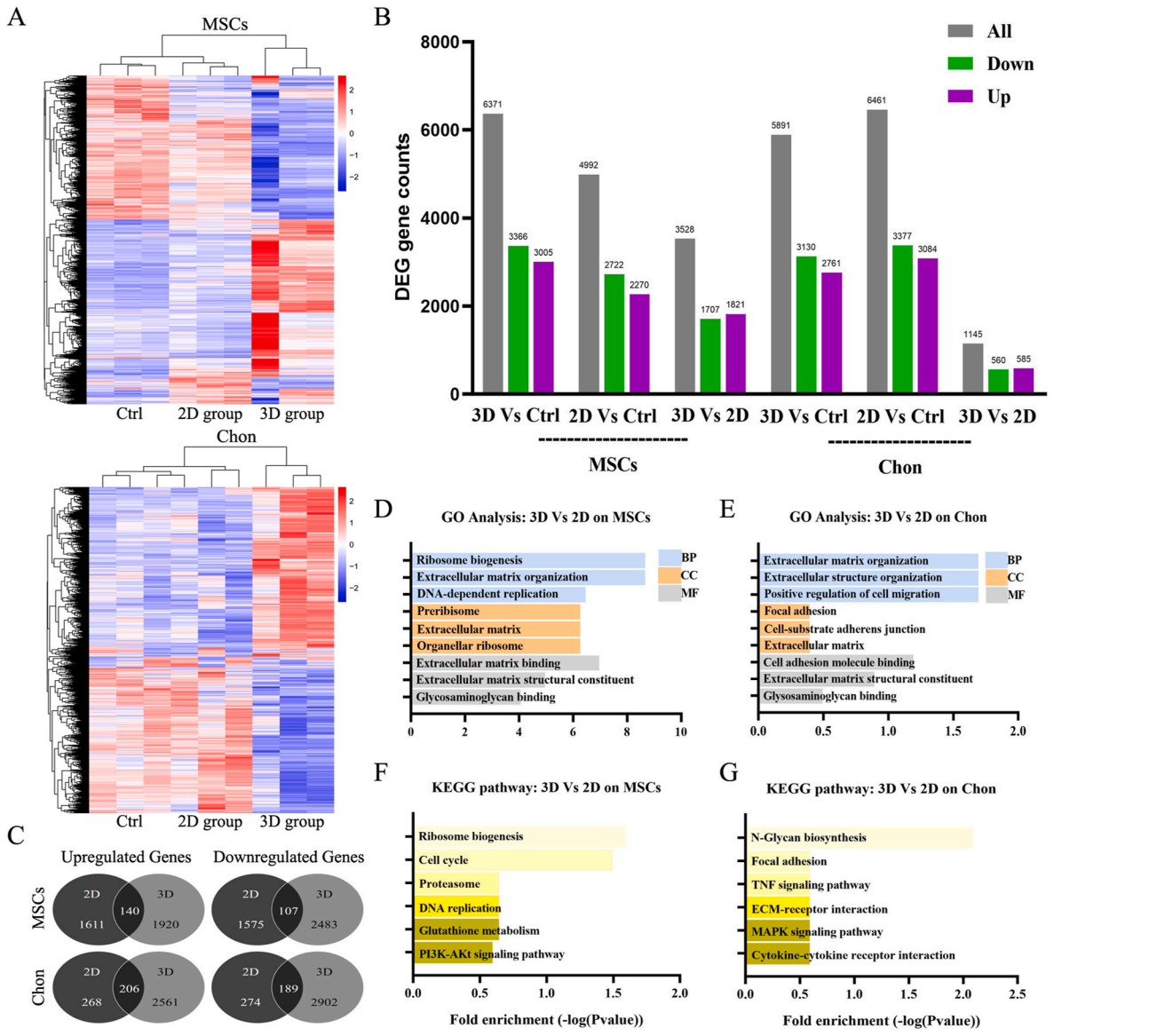

Fig. 6. RNA-seq analysis of co-cultured chondrocytes and MSCs. (A) Heatmaps of differentially expressed mRNA levels for MSCs and chondrocytes from the 3D and 2D groups. (B) Upregulated and downregulated genes from differentially expressed genes (DEGs) in MSCs and chondrocytes. (C) Venn diagrams showing the number of significantly altered genes (≥2-fold difference; upregulated and downregulated) in MSCs and chondrocytes. (D, E) GO enrichment analysis of upregulated genes in MSCs and chondrocytes (3D group vs 2D group). (F, G) KEGG pathway analysis using DAVID for upregulated genes in MSCs and chondrocytes (3D group vs 2D group). BP: Biological Process; CC: Cellular Component; MF: Molecular Function.

(Fig. 6B). As shown by Venn diagrams, the overlapping upregulated and downregulated genes between 2D and 3D groups in MSCs were 140 and 107, respectively, while those for chondrocytes were 206 and 189 (Fig. 6C). Heap map clustering based on genes with $p < 0.05$ and $\log_2$FC above or below cutoff (>1, <-1) showed that the 3D group had an overall response reflective of significant changes in the transcriptomic profile of co-cultured cells. Volcano plots of the upregulated and downregulated DEGs in MSCs and chondrocytes are illustrated in the supplementary data (Fig. S3).

GO enrichment analysis was performed for the upregulated genes in MSCs and chondrocytes. The majority of enriched biological processes in MSCs in the 3D compared to 2D group were related to ribosome biogenesis, DNA replication, extracellular matrix organization, regulation of cell cycle, extracellular matrix binding, collagen binding, peribosome, and extracellular matrix structural constituent (Fig. 6D, S4A, B). Similar biological processes have been reported in other studies on early chondrogenic induction in MSCs [46]. For chondrocytes co-cultured with MSCs, differences between the 3D compared to 2D group were related more closely to cartilage development, including processes on the regulation of extracellular matrix, focal adhesion, positive regulation of cell migration, and glycosaminoglycan binding (Fig. 6E, S4C, D). These results suggest that in the co-culture system, MSCs cultured in 3D can promote better initiation of MSC chondrogenesis and phenotypic maintenance in the co-cultured chondrocytes compared to MSCs cultured in 2D.

KEGG pathway analyses for MSCs and chondrocytes were performed using the Database for Annotation, Visualization and Integrated Discovery (DAVID). The top pathways of upregulated genes in the 3D compared to 2D group for MSCs and chondrocytes are shown. The “cell cycle” and “DNA replication” pathways were reported for MSC proliferation. Furthermore, KEGG clusters related to “ribosome biogenesis” and “PI3K-Akt signaling pathway” were greatly induced during MSC chondrogenesis in the 3D group (Fig. 6F, S4E, F). These results matched previous investigations reporting an increase in cell proliferation during

chondrogenesis [47]. In chondrocytes, the results showed important pathways in phenotype preservation relating to "focal adhesion", "MAPK signaling pathway", and "cytokine-cytokine receptor interaction" (Fig. 6G, S4G, H). "N-Glycan biosynthesis" was also enriched in chondrocytes co-cultured with MSCs in the 3D group, which was consistent with other reports demonstrating positive effects of this pathway in the maintenance of articular cartilage [48].

4. Discussion

In this study, we used both an *in vivo* ACL transection OA model and an *in vitro* co-culture model to investigate the therapeutic effects of MSC-laden microniches in a chronic OA environment. Current clinical evidence points to the benefits of repeated intra-articular injections of therapeutic substances, such as HA and MSCs, instead of a single dose [24], which while more effective is also associated with a higher risk of infection and other complications [27]. Using the *in vivo* model, we demonstrated that microniches may allow a single low dose of MSCs to achieve similar restorative effects as repeated high doses of MSCs, as indicated by radiological, μ-CT and histological analyses. Using the *in vitro* model, we illustrated potential molecular mechanisms of interactions between MSCs and host chondrocytes in an OA environment, and investigated the contributions of cell delivery in microniches through secretome and transcriptome analyses.

The loss of proteoglycans and loosening of the collagen meshwork constitute major ECM changes in OA disease progression. It has been reported that MSCs can promote cartilage preservation and/or accelerate cartilage restoration due to their self-renewal capacity, trophic secretory functions, immunomodulation properties, and ability to override the HLA barrier to allow for allogeneic transplantation [24,49–52]. A number of clinical trials have been conducted whereby MSC injections were used to treat knee OA, but these have reported some inconsistent or even contradictory results [53,54]. While it is generally believed that MSC therapy has dose-dependent effects and larger quantities of cells are more effective, further high-quality evidence is needed to confirm the long-term safety and clinical advantages of high-dose MSC injections. One of the caveats of using high-dose MSC injections is that the cells often undergo repeated expansion in 2D culture, which is not an ideal method for maintaining their stemness and phenotypic characteristics. 3D culture is known to provide cells with the ability to establish a biomimetic hierarchical structure that facilitates better maintenance of stemness and viability [55,56]. However, the development of a stable and efficient method for the 3D culture of MSCs in scale-up applications has been a challenge. Our injectable gelatin microcarriers, which were used in this study provides a possible cell delivery platform to address this challenge, by providing a 3D substrate to allow for optimal cell anchorage, phenotypic regulation and proliferation that then contribute to their improved therapeutic functions [19]. These microcarriers are made from clinically applicable gelatin, which provides inherent cell adhesion motifs, and their 3D microporous structure provides MSCs with a native microenvironment to improve cell retention and therapeutic functions following *in vivo* injection [34].

We performed a single injection of MSC-laden microniches into an experimentally-induced ACL transection model of knee OA. ACL transection surgery in rats is used to model human post-traumatic OA, by producing joint instability and altering load-bearing in the knee. In this model, there is a clear relationship between ACL transection as the disease-initiating event and the development of OA-associated pathology [57,58]. Treatment groups were injected at 6 weeks following the initial surgery, the time at which post-traumatic OA would have developed and would progress to severe OA without intervention. Through imaging and histological analyses, we showed that microniches loaded with a low dose of MSCs achieved comparable reparative effects in a physiologically-relevant *in vivo* model of OA at 6 weeks after intervention relative to repeated high-dose injections of free MSCs, which were far superior to the results achieved using repeated HA injections. This approach of using MSC-laden microniches may provide an alternative to the need of producing large amounts of MSCs for large-scale clinical use, which may not be economically or practically viable due to the limited sources of primary MSCs and the costs of cell harvesting and expansion processes [59,60]. Nevertheless, it is important to recognize that these injectable microniches would be more suitable for treating early-stage OA with cartilage deterioration as the main pathological characteristic, rather than late-stage OA with moderate to large defect areas. OA is defined by the main pathological characteristics of cartilage deterioration, aberrant osteophytes or synovitis, and subchondral bone changes. In early-stage OA, cartilage deterioration would be the most common cause of knee pain and joint instability, which may benefit from early intervention such as oral medicine, and HA or MSC injections. For late-stage OA with large-scale lesions and tissue degeneration on a whole-joint level, joint arthroplasty would be the last choice for treatment.

Cell-cell interactions are implicated in a plethora of biological phenomena spanning embryogenesis, tissue morphogenesis, and repair. In the context of joint repair, the co-culture of expanded MSCs with primary chondrocytes or cartilage explants offers an ideal approach to investigate the specific paracrine functions of MSCs that may contribute to their therapeutic effects. Co-culture models can be set up to mimic the *in vivo* physiological or pathological joint environment, where the transplanted MSCs would be surrounded by, but not be in direct contact with, native chondrocytes residing within the host cartilage [40,61,62]. In this study, we established co-cultures of chondrocytes with MSCs in transwells, either growing in microniches or as a monolayer. Gene and protein expression results showed that MSCs in microniches increased the expression of chondrogenic markers in both MSCs and chondrocytes, suggesting that MSCs growing in a 3D compared to 2D environment are more responsive to chondrogenic signals, and promote better maintenance of phenotype in the co-cultured chondrocytes. Moreover, MSCs can be activated by inflammatory factors to directly suppress immune cells [63]. In our co-cultures supplemented with IL-1β, secretome analysis showed that the expression of inflammatory markers such as IL-6R was greatly downregulated in the co-culture supernatants with 3D MSCs compared to 2D MSCs. On the other hand, the greater upregulation of GM-CSF in the 3D group was associated with a possible role in cartilage repair [64,65]. Taken together, these findings suggest that MSCs grown in 3D microniches have paracrine functions that may be more effective at reducing inflammation and increasing cartilage repair in OA compared to those cultured in monolayer. As a cell delivery vehicle, if these MSC-laden microniches are applied in a clinical setting, we expect the MSCs to exert their therapeutic effects in OA joints mainly through paracrine functions and their immunomodulatory effects, which are elevated through their retainment within the microniches. We would not expect the MSCs to be released from the microniches, or to colonize cartilage defects and directly differentiate into new tissue.

Previous studies on co-culture systems involving MSCs and chondrocytes mainly focused on their bi-directional effects on gene and protein expression in the context of chondrogenesis. For instance, MSCs in co-culture have been found to enhance chondrocyte proliferation and ECM synthesis [66], while the chondrocytes can simultaneously promote the differentiation of MSCs [62,67]. Morphogens or other factors secreted by chondrocytes can contribute to reducing hypertrophy and increasing chondrogenic differentiation in MSCs [40,41,68], possibly through the transfer of extracellular vesicles [38,69]. However, the possible interactions between MSCs and chondrocytes in a pathological joint environment have been rarely investigated using co-culture models. The results from a previous study suggested that OA chondrocytes could promote chondrogenic differentiation of MSCs while downregulating type I and X collagen expression. This effect could not be achieved using conditioned medium from primary (P0) OA chondrocytes or co-culturing with passaged (P1) OA chondrocytes, indicating the importance of intercellular communication and chondrocyte phenotype for inducing chondrogenic differentiation of MSCs [40]. In

this study, we for the first time investigated the whole transcriptomic profile of co-cultured human MSCs and chondrocytes in an inflammatory environment simulating knee OA stimulated by IL-1β. We found different transcriptomic profiles in both MSCs and chondrocytes when comparing between the 3D and 2D co-cultured groups. MSCs in 3D microniches co-cultured with chondrocytes showed GO terms relating to ribosome biogenesis, ECM organization, and positive regulation of cell migration and glycosaminoglycan binding, processes which were similar to those encountered in MSC chondrogenesis [70]. Chondrocytes in the 3D group showed significant variations in gene expression relating to cellular processes, ECM, and signal transduction, suggesting a comprehensive response that was also observed in other studies using rabbit chondrocytes [71]. A number of cartilage-related GO terms for both MSCs and chondrocytes in the 3D group suggested that MSCs cultured in microniches had greater potential to maintain *in vitro* chondrogenesis and maintenance of the original chondrocyte phenotype. KEGG pathway analysis showed enrichment for ribosome biogenesis, cell cycle, and PI3K-Akt signaling pathway in 3D MSCs. The enrichment of PI3K-Akt signaling pathway possibly points to a mechanism by which MSCs in microniches may undergo increased proliferation and improve the repair of OA injury [72–74]. Chondrocytes in the 3D group showed enrichment for focal adhesion and N-Glycan biosynthesis pathway, possibly suggesting better phenotype maintenance. The differences in transcriptomic profile of MSCs in 3D culture compared to 2D, which may broadly contribute to their paracrine functions and therapeutic effects, may be attributed to improved cell adhesion, proliferation and ECM deposition [28,75].

There are some limitations in our study that will be addressed in follow-up investigations. First, culturing primary chondrocytes in monolayer in the co-culture models is not optimal for maintaining their phenotypic characteristics. However, this was the most efficient method for reducing the number of variables, while isolating the interactions between chondrocytes and MSCs for secretome and transcriptome analyses. To establish a more physiologically relevant *in vitro* co-culture model, culturing the chondrocytes in pellet form or seeded inside a biomaterial should be investigated in future studies. The use of patient-matched chondrocytes and MSCs should also be considered. Second, while the transwell co-culture model in our study revealed complex and compelling cell-cell interactions, we were unable to perform analyses relating to the nature of the transfer cargo between cell types, their transport mechanisms, and variations between chondrocytes in different zones of articular cartilage. These factors may all contribute to the repair mechanisms of MSCs in a pathological joint environment and warrant further investigation. Last, our *in vivo* experiment was performed in a small rodent model, which would not be representative of reparative effects in humans. Studies in larger animals will be required before the clinical relevance of using MSC-laden microniches to treat patients with knee OA can be determined.

5. Conclusion

MSC-laden microniches grown in spinner flasks loaded with a low cell dose and delivered through a single injection achieved similar reparative effects in an *in vivo* model of post-traumatic OA as repeated high dose injections of MSCs. This in itself shows the advantages of MSC-laden microniches, by significantly reducing the cell numbers and injection frequency required to demonstrate a therapeutic effect. The elevated therapeutic effects of MSCs when delivered through microniches may be reflective of their increased anti-inflammatory and trophic functions when grown in a 3D environment. Chondrocytes in monolayer and MSCs in microniches or monolayer, grown in co-culture showed bi-directional interactions and mutually beneficial effects that were relevant for the potential use of MSC-laden microniches as future therapeutics for the treatment of OA.

Funding

This study was supported by grants from the National Natural Science Foundation of China (No. 81730067, 81802204), China Postdoctoral Science Foundation (2020M671453), and the National Health and Medical Research Council (Australia; GNT1120249).

CRediT authorship contribution statement

Bin Wang: conception and design, materials fabrication, collection and assembly data, data analysis and interpretation, manuscript writing, final approval of manuscript. **Wei Liu:** conception and design, materials fabrication, collection and assembly data, data analysis and interpretation, manuscript writing, final approval of manuscript. **Jiao Jiao Li:** conception and design, manuscript writing, final approval of manuscript. **Senlin Chai:** conception and design, manuscript writing, final approval of manuscript. **Dan Xing:** conception and design, manuscript writing, final approval of manuscript. **Hongsheng Yu:** conception and design, manuscript writing, final approval of manuscript. **Yuanyuan Zhang:** data interpretation, manuscript writing and final approval of manuscript. **Wenjin Yan:** data interpretation, manuscript writing and final approval of manuscript. **Zhihong Xu:** manuscript writing. **Bin Zhao:** manuscript writing. **Yanan Du:** conception and design, manuscript writing, final approval of manuscript. **Qing Jiang:** conception and design, manu-script writing, final approval of manuscript.

Declaration of competing interest

Wei Liu is employed by Beijing CytoNiche Biotechnology Co. Ltd. The other authors declare no financial and personal relationships with other people or organizations that can inappropriately influence our work.

Acknowledgements

We gratefully acknowledge Dr Xiaojun Yan for their assistance in preparing the microcarriers and providing technical support. We also thank Dr Chunxiao Qi from the Nankai University for technical assistance.

Appendix A. Supplementary data

Supplementary data to this article can be found online at https://doi.org/10.1016/j.bioactmat.2021.05.029.

References

[1] E.A. Makris, A.H. Gomoll, K.N. Malizos, J.C. Hu, K.A. Athanasiou, Repair and tissue engineering techniques for articular cartilage, Nat. Rev. Rheumatol. 11 (1) (2015) 21–34, https://doi.org/10.1038/nrrheum.2014.157.

[2] S. Safiri, A.A. Kolahi, E. Smith, C. Hill, D. Bettampadi, M.A. Mansournia, D. Hoy, A. Ashrafi-Asgarabad, M. Sepidarkish, A. Almasi-Hashiani, G. Collins, J. Kaufman, M. Qorbani, M. Moradi-Lakeh, A.D. Woolf, F. Guillemin, L. March, M. Cross, Global, regional and national burden of osteoarthritis 1990-2017: a systematic analysis of the Global Burden of Disease Study 2017, Ann. Rheum. Dis. 79 (6) (2020) 819–828, https://doi.org/10.1136/annrheumdis-2019-216515.

[3] H. Long, X. Zeng, Q. Liu, H. Wang, T. Vos, Y. Hou, C. Lin, Y. Qiu, K. Wang, D. Xing, Y. Zhang, M. Zhou, J. Lin, Burden of osteoarthritis in China, 1990–2017: findings from the global burden of disease study 2017, Lancet Rheumatol. 2 (3) (2020) e164–e172, https://doi.org/10.1016/S2665-9913(19)30145-6.

[4] R.R. Bannuru, M.C. Osani, E.E. Vaysbrot, N.K. Arden, K. Bennell, S.M.A. Bierma-Zeinstra, V.B. Kraus, L.S. Lohmander, J.H. Abbott, M. Bhandari, F.J. Blanco, R. Espinosa, I.K. Haugen, J. Lin, L.A. Mandl, E. Moilanen, N. Nakamura, L. Snyder-Mackler, T. Trojian, M. Underwood, T.E. McAlindon, OARSI guidelines for the non-surgical management of knee, hip, and polyarticular osteoarthritis, Osteoarthritis Cartilage 27 (11) (2019) 1578–1589, https://doi.org/10.1016/j.joca.2019.06.011.

[5] B. McGrory, K. Weber, J.A. Lynott, J.C. Richmond, C.M. Davis 3rd, A. Yates Jr., A. F. Kamath, V. Dasa, G.A. Brown, T.L. Gerlinger, T. Villanueva, S. Piva, J. Hebl, D. Jevsevar, K.G. Shea, K.J. Bozic, W. Shaffer, D. Cummins, J.N. Murray, P. Donnelly, N. Patel, B. Brenton, P. Shores, A. Woznica, E. Linskey, K. Sevarino, S. American Academy of Orthopaedic, The American academy of orthopaedic surgeons evidence-based clinical practice guideline on surgical management of

osteoarthritis of the knee, J. Bone Joint Surg. Am. 98 (8) (2016) 688–692, https://doi.org/10.2106/JBJS.15.01311.
[6] G.A. Hawker, S. Mian, K. Bednis, I. Stanaitis, Osteoarthritis year 2010 in review: non-pharmacologic therapy, Osteoarthritis Cartilage 19 (4) (2011) 366–374, https://doi.org/10.1016/j.joca.2011.01.021.
[7] R.H. Hunt, A. Lanas, D.O. Stichtenoth, C. Scarpignato, Myths and facts in the use of anti-inflammatory drugs, Ann. Med. 41 (6) (2009) 423–437, https://doi.org/10.1080/07853890902887295.
[8] S.T. Skou, E.M. Roos, M.B. Laursen, A randomized, controlled trial of total knee replacement, N. Engl. J. Med. 374 (7) (2016) 692, https://doi.org/10.1056/NEJMc1514794.
[9] E. Mianehsaz, H.R. Mirzaei, M. Mahjoubin-Tehran, A. Rezaee, R. Sahebnasagh, M. H. Pourhanifeh, H. Mirzaei, M.R. Hamblin, Mesenchymal stem cell-derived exosomes: a new therapeutic approach to osteoarthritis? Stem Cell Res. Ther. 10 (1) (2019) 340, https://doi.org/10.1186/s13287-019-1445-0.
[10] A. Trounson, C. McDonald, Stem cell therapies in clinical trials: progress and challenges, Cell Stem Cell 17 (1) (2015) 11–22, https://doi.org/10.1016/j.stem.2015.06.007.
[11] J. Wu, L. Kuang, C. Chen, J. Yang, W.N. Zeng, T. Li, H. Chen, S. Huang, Z. Fu, J. Li, R. Liu, Z. Ni, L. Chen, L. Yang, miR-100-5p-abundant exosomes derived from infrapatellar fat pad MSCs protect articular cartilage and ameliorate gait abnormalities via inhibition of mTOR in osteoarthritis, Biomaterials 206 (2019) 87–100, https://doi.org/10.1016/j.biomaterials.2019.03.022.
[12] H. Mirzaei, A. Sahebkar, L.S. Sichani, A. Moridikia, S. Nazari, J. Sadri Nahand, H. Salehi, J. Stenvang, A. Masoudifar, H.R. Mirzaei, M.R. Jaafari, Therapeutic application of multipotent stem cells, J. Cell. Physiol. 233 (4) (2018) 2815–2823, https://doi.org/10.1002/jcp.25990.
[13] C. Mason, D.A. Brindley, E.J. Culme-Seymour, N.L. Davie, Cell therapy industry: billion dollar global business with unlimited potential, Regen. Med. 6 (3) (2011) 265–272, https://doi.org/10.2217/rme.11.28.
[14] K. Johnson, S. Zhu, M.S. Tremblay, J.N. Payette, J. Wang, L.C. Bouchez, S. Meeusen, A. Althage, C.Y. Cho, X. Wu, P.G. Schultz, A stem cell-based approach to cartilage repair, Science 336 (6082) (2012) 717–721, https://doi.org/10.1126/science.1215157.
[15] R. Moradian Tehrani, J. Verdi, M. Noureddini, R. Salehi, R. Salarinia, M. Mosalaei, M. Simonian, B. Alani, M.R. Ghiasi, M.R. Jaafari, H.R. Mirzaei, H. Mirzaei, Mesenchymal stem cells: a new platform for targeting suicide genes in cancer, J. Cell. Physiol. 233 (5) (2018) 3831–3845, https://doi.org/10.1002/jcp.26094.
[16] B.O. Diekman, F. Guilak, Stem cell-based therapies for osteoarthritis: challenges and opportunities, Curr. Opin. Rheumatol. 25 (1) (2013) 119–126, https://doi.org/10.1097/BOR.0b013e32835aa28d.
[17] Y.H. Chang, H.W. Liu, K.C. Wu, D.C. Ding, Mesenchymal stem cells and their clinical applications in osteoarthritis, Cell Transplant. 25 (5) (2016) 937–950, https://doi.org/10.3727/096368915X690288.
[18] M. Morille, K. Toupet, C.N. Montero-Menei, C. Jorgensen, D. Noel, PLGA-based microcarriers induce mesenchymal stem cell chondrogenesis and stimulate cartilage repair in osteoarthritis, Biomaterials 88 (2016) 60–69, https://doi.org/10.1016/j.biomaterials.2016.02.022.
[19] X. Yan, K. Zhang, Y. Yang, D. Deng, C. Lyu, H. Xu, W. Liu, Y. Du, Dispersible and dissolvable porous microcarrier tablets enable efficient large-scale human mesenchymal stem cell expansion, Tissue Eng. C Methods 26 (5) (2020) 263–275, https://doi.org/10.1089/ten.TEC.2020.0039.
[20] N. Parmar, R. Ahmadi, R.M. Day, A novel method for differentiation of human mesenchymal stem cells into smooth muscle-like cells on clinically deliverable thermally induced phase separation microspheres, Tissue Eng. C Methods 21 (4) (2015) 404–412, https://doi.org/10.1089/ten.TEC.2014.0431.
[21] C. Feng, X. Luo, N. He, H. Xia, X. Lv, X. Zhang, D. Li, F. Wang, J. He, L. Zhang, X. Lin, L. Lin, H. Yin, J. He, J. Wang, W. Cao, R. Wang, G. Zhou, W. Wang, Efficacy and persistence of allogeneic adipose-derived mesenchymal stem cells combined with hyaluronic acid in osteoarthritis after intra-articular injection in a sheep model, Tissue Eng. 24 (3–4) (2018) 219–233, https://doi.org/10.1089/ten.TEA.2017.0039.
[22] G. Desando, I. Bartolotti, C. Cavallo, A. Schiavinato, C. Secchieri, E. Kon, G. Filardo, M. Paro, B. Grigolo, Short-term homing of hyaluronan-primed cells: therapeutic implications for osteoarthritis treatment, Tissue Eng. C Methods 24 (2) (2018) 121–133, https://doi.org/10.1089/ten.TEC.2017.0336.
[23] N. Ozeki, T. Muneta, H. Koga, Y. Nakagawa, M. Mizuno, K. Tsuji, Y. Mabuchi, C. Akazawa, E. Kobayashi, K. Matsumoto, K. Futamura, T. Saito, I. Sekiya, Not single but periodic injections of synovial mesenchymal stem cells maintain viable cells in knees and inhibit osteoarthritis progression in rats, Osteoarthritis Cartilage 24 (6) (2016) 1061–1070, https://doi.org/10.1016/j.joca.2015.12.018.
[24] J. Matas, M. Orrego, D. Amenabar, C. Infante, R. Tapia-Limonchi, M.I. Cadiz, F. Alcayaga-Miranda, P.L. Gonzalez, E. Muse, M. Khoury, F.E. Figueroa, F. Espinoza, Umbilical cord-derived mesenchymal stromal cells (MSCs) for knee osteoarthritis: repeated MSC dosing is superior to a single MSC dose and to hyaluronic acid in a controlled randomized phase I/II trial, Stem Cells Transl. Med. 8 (3) (2019) 215–224, https://doi.org/10.1002/sctm.18-0053.
[25] T. Enomoto, R. Akagi, Y. Ogawa, S. Yamaguchi, H. Hoshi, T. Sasaki, Y. Sato, R. Nakagawa, S. Kimura, S. Ohtori, T. Sasho, Timing of intra-articular injection of synovial mesenchymal stem cells affects cartilage restoration in a partial thickness cartilage defect model in rats, Cartilage 11 (1) (2020) 122–129, https://doi.org/10.1177/1947603518786542.
[26] C.H. Jo, J.W. Chai, E.C. Jeong, S. Oh, J.S. Shin, H. Shim, K.S. Yoon, Intra-articular injection of mesenchymal stem cells for the treatment of osteoarthritis of the knee: a 2-year follow-up study, Am. J. Sports Med. 45 (12) (2017) 2774–2783, https://doi.org/10.1177/0363546517716641.
[27] F. Migliorini, B. Rath, G. Colarossi, A. Driessen, M. Tingart, M. Niewiera, J. Eschweiler, Improved outcomes after mesenchymal stem cells injections for knee osteoarthritis: results at 12-months follow-up: a systematic review of the literature, Arch. Orthop. Trauma Surg. 140 (7) (2020) 853–868, https://doi.org/10.1007/s00402-019-03267-8.
[28] Y. Li, W. Liu, F. Liu, Y. Zeng, S. Zuo, S. Feng, C. Qi, B. Wang, X. Yan, A. Khademhosseini, J. Bai, Y. Du, Primed 3D injectable microniches enabling low-dosage cell therapy for critical limb ischemia, Proc. Natl. Acad. Sci. U. S. A. 111 (37) (2014) 13511–13516, https://doi.org/10.1073/pnas.1411295111.
[29] W. Liu, Y. Li, Y. Zeng, X. Zhang, J. Wang, L. Xie, X. Li, Y. Du, Microcryogels as injectable 3-D cellular microniches for site-directed and augmented cell delivery, Acta Biomater. 10 (5) (2014) 1864–1875, https://doi.org/10.1016/j.actbio.2013.12.008.
[30] D. Xing, W. Liu, J.J. Li, L. Liu, A. Guo, B. Wang, H. Yu, Y. Zhao, Y. Chen, Z. You, C. Lyu, W. Li, A. Liu, Y. Du, J. Lin, Engineering 3D functional tissue constructs using self-assembling cell-laden microniches, Acta Biomater. (2020), https://doi.org/10.1016/j.actbio.2020.07.058.
[31] D. Xing, W. Liu, B. Wang, J.J. Li, Y. Zhao, H. Li, A. Liu, Y. Du, J. Lin, Intra-articular injection of cell-laden 3D microcryogels empower low-dose cell therapy for osteoarthritis in a rat model, Cell Transplant. 29 (2020), https://doi.org/10.1177/0963689720932142, 963689720932142.
[32] P. Di Nardo, D. Singla, R.K. Li, The challenges of stem cell therapy, Can. J. Physiol. Pharmacol. 90 (3) (2012) 273–274, https://doi.org/10.1139/y2012-016.
[33] H. Tavassoli, S.N. Alhosseini, A. Tay, P.P.Y. Chan, S.K. Weng Oh, M.E. Warkiani, Large-scale production of stem cells utilizing microcarriers: a biomaterials engineering perspective from academic research to commercialized products, Biomaterials 181 (2018) 333–346, https://doi.org/10.1016/j.biomaterials.2018.07.016.
[34] H. Yu, Z. You, X. Yan, W. Liu, Z. Nan, D. Xing, C. Huang, Y. Du, TGase-enhanced microtissue assembly in 3D-printed-template-scaffold (3D-MAPS) for large tissue defect reparation, Adv. Healthc. Mater. (2020), e2000531, https://doi.org/10.1002/adhm.202000531.
[35] P. Agrawal, K. Pramanik, A. Biswas, R. Ku Patra, In vitro cartilage construct generation from silk fibroin- chitosan porous scaffold and umbilical cord blood derived human mesenchymal stem cells in dynamic culture condition, J. Biomed. Mater. Res. 106 (2) (2018) 397–407, https://doi.org/10.1002/jbm.a.36253.
[36] P. Agrawal, K. Pramanik, Enhanced chondrogenic differentiation of human mesenchymal stem cells in silk fibroin/chitosan/glycosaminoglycan scaffolds under dynamic culture condition, Differentiation 110 (2019) 36–48, https://doi.org/10.1016/j.diff.2019.09.004.
[37] S. Sulaiman, S.R. Chowdhury, M.B. Fauzi, R.A. Rani, N.H.M. Yahaya, Y. Tabata, Y. Hiraoka, R. Binti Haji Idrus, N. Min Hwei, 3D culture of MSCs on a gelatin microsphere in a dynamic culture system enhances chondrogenesis, Int. J. Mol. Sci. 21 (8) (2020), https://doi.org/10.3390/ijms21082688.
[38] M. Kim, D.R. Steinberg, J.A. Burdick, R.L. Mauck, Extracellular vesicles mediate improved functional outcomes in engineered cartilage produced from MSC/chondrocyte cocultures, Proc. Natl. Acad. Sci. U. S. A. 116 (5) (2019) 1569–1578, https://doi.org/10.1073/pnas.1815447116.
[39] V.V. Meretoja, R.L. Dahlin, F.K. Kasper, A.G. Mikos, Enhanced chondrogenesis in co-cultures with articular chondrocytes and mesenchymal stem cells, Biomaterials 33 (27) (2012) 6362–6369, https://doi.org/10.1016/j.biomaterials.2012.05.042.
[40] A. Aung, G. Gupta, G. Majid, S. Varghese, Osteoarthritic chondrocyte-secreted morphogens induce chondrogenic differentiation of human mesenchymal stem cells, Arthritis Rheum. 63 (1) (2011) 148–158, https://doi.org/10.1002/art.30086.
[41] L. Bian, D.Y. Zhai, R.L. Mauck, J.A. Burdick, Coculture of human mesenchymal stem cells and articular chondrocytes reduces hypertrophy and enhances functional properties of engineered cartilage, Tissue Eng. 17 (7–8) (2011) 1137–1145, https://doi.org/10.1089/ten.tea.2010.0531.
[42] K.P.H. Pritzker, S. Gay, S.A. Jimenez, K. Ostergaard, J.P. Pelletier, P.A. Revell, D. Salter, W.B. van den Berg, Osteoarthritis cartilage histopathology: grading and staging, Osteoarthritis Cartilage 14 (1) (2006) 13–29, https://doi.org/10.1016/j.joca.2005.07.014.
[43] H.J. Mankin, L. Lippiello, Biochemical and metabolic abnormalities in articular cartilage from osteo-arthritic human hips, J. Bone Joint Surg. Am. 52 (1970).
[44] X.-d. Gu, L. Wei, P.-c. Li, X.-d. Che, R.-p. Zhao, P.-f. Han, J.-g. Lu, X.-c. Wei, Adenovirus-mediated transduction with Histone Deacetylase 4 ameliorates disease progression in an osteoarthritis rat model, Int. Immunopharm. 75 (2019) 105752, https://doi.org/10.1016/j.intimp.2019.105752.
[45] V. Bunpetch, X. Zhang, T. Li, J. Lin, E.P. Maswikiti, Y. Wu, D. Cai, J. Li, S. Zhang, C. Wu, H. Ouyang, Silicate-based bioceramic scaffolds for dual-lineage regeneration of osteochondral defect, Biomaterials 192 (2019) 323–333, https://doi.org/10.1016/j.biomaterials.2018.11.025.
[46] P.A. Trainor, A.E. Merrill, Ribosome biogenesis in skeletal development and the pathogenesis of skeletal disorders, Biochim. Biophys. Acta 1842 (6) (2014) 769–778, https://doi.org/10.1016/j.bbadis.2013.11.010.
[47] F. Beier, R.F. Loeser, Biology and pathology of Rho GTPase, PI-3 kinase-Akt, and MAP kinase signaling pathways in chondrocytes, J. Cell. Biochem. 110 (3) (2010) 573–580, https://doi.org/10.1002/jcb.22604.
[48] A. Urita, T. Matsuhashi, T. Onodera, H. Nakagawa, M. Hato, M. Amano, N. Seito, A. Minami, S. Nishimura, N. Iwasaki, Alterations of high-mannose type N-glycosylation in human and mouse osteoarthritis cartilage, Arthritis Rheum. 63 (11) (2011) 3428–3438, https://doi.org/10.1002/art.30584.
[49] X. Fu, G. Liu, A. Halim, Y. Ju, Q. Luo, A.G. Song, Mesenchymal stem cell migration and tissue repair, Cells 8 (8) (2019), https://doi.org/10.3390/cells8080784.
[50] D.C. Ding, H.L. Chou, Y.H. Chang, W.T. Hung, H.W. Liu, T.Y. Chu, Characterization of HLA-G and related immunosuppressive effects in human umbilical cord stroma-

derived stem cells, Cell Transplant. 25 (2) (2016) 217–228, https://doi.org/10.3727/096368915X688182.
[51] S.M. Richardson, G. Kalamegam, P.N. Pushparaj, C. Matta, A. Memic, A. Khademhosseini, R. Mobasheri, F.L. Poletti, J.A. Hoyland, A. Mobasheri, Mesenchymal stem cells in regenerative medicine: focus on articular cartilage and intervertebral disc regeneration, Methods 99 (2016) 69–80, https://doi.org/10.1016/j.ymeth.2015.09.015.
[52] Y.B. Park, C.W. Ha, C.H. Lee, Y.C. Yoon, Y.G. Park, Cartilage regeneration in osteoarthritic patients by a composite of allogeneic umbilical cord blood-derived mesenchymal stem cells and hyaluronate hydrogel: results from a clinical trial for safety and proof-of-concept with 7 Years of extended follow-up, Stem Cells Transl. Med. 6 (2) (2017) 613–621, https://doi.org/10.5966/sctm.2016-0157.
[53] Y.S. Kim, Y.J. Choi, Y.G. Koh, Mesenchymal stem cell implantation in knee osteoarthritis: an assessment of the factors influencing clinical outcomes, Am. J. Sports Med. 43 (9) (2015) 2293–2301, https://doi.org/10.1177/0363546515588317.
[54] S. Lopa, A. Colombini, M. Moretti, L. de Girolamo, Injective mesenchymal stem cell-based treatments for knee osteoarthritis: from mechanisms of action to current clinical evidences, Knee Surg. Sports Traumatol. Arthrosc. 27 (6) (2019) 2003–2020, https://doi.org/10.1007/s00167-018-5118-9.
[55] C. Zhang, B. Xie, Y. Zou, D. Zhu, L. Lei, D. Zhao, H. Nie, Zero-dimensional, one-dimensional, two-dimensional and three-dimensional biomaterials for cell fate regulation, Adv. Drug Deliv. Rev. 132 (2018) 33–56, https://doi.org/10.1016/j.addr.2018.06.020.
[56] N.E. Ryu, S.H. Lee, H. Park, Spheroid culture system methods and applications for mesenchymal stem cells, Cells 8 (12) (2019), https://doi.org/10.3390/cells8121620.
[57] H. Fang, F. Beier, Mouse models of osteoarthritis: modelling risk factors and assessing outcomes, Nat. Rev. Rheumatol. 10 (7) (2014) 413–421, https://doi.org/10.1038/nrrheum.2014.46.
[58] D. Xing, J. Kwong, Z. Yang, Y. Hou, W. Zhang, B. Ma, J. Lin, Intra-articular injection of mesenchymal stem cells in treating knee osteoarthritis: a systematic review of animal studies, Osteoarthritis Cartilage 26 (4) (2018) 445–461, https://doi.org/10.1016/j.joca.2018.01.010.
[59] I. Martin, P.J. Simmons, D.F. Williams, Manufacturing challenges in regenerative medicine, Sci. Transl. Med. 6 (232) (2014) 232fs16, https://doi.org/10.1126/scitranslmed.3008558.
[60] Y. Haraguchi, T. Shimizu, M. Yamato, T. Okano, Concise review: cell therapy and tissue engineering for cardiovascular disease, Stem Cells Transl. Med. 1 (2) (2012) 136–141, https://doi.org/10.5966/sctm.2012-0030.
[61] H.J. Diao, C.W. Yeung, C.H. Yan, G.C. Chan, B.P. Chan, Bidirectional and mutually beneficial interactions between human mesenchymal stem cells and osteoarthritic chondrocytes in micromass co-cultures, Regen. Med. 8 (3) (2013) 257–269, https://doi.org/10.2217/rme.13.22.
[62] C. Acharya, A. Adesida, P. Zajac, M. Mumme, J. Riesle, I. Martin, A. Barbero, Enhanced chondrocyte proliferation and mesenchymal stromal cells chondrogenesis in coculture pellets mediate improved cartilage formation, J. Cell. Physiol. 227 (1) (2012) 88–97, https://doi.org/10.1002/jcp.22706.
[63] A.T. Wang, Y. Feng, H.H. Jia, M. Zhao, H. Yu, Application of mesenchymal stem cell therapy for the treatment of osteoarthritis of the knee: a concise review, World J. Stem Cell. 11 (4) (2019) 222–235, https://doi.org/10.4252/wjsc.v11.i4.222.
[64] M. Brittberg, E. Sjogren-Jansson, M. Thornemo, B. Faber, A. Tarkowski, L. Peterson, A. Lindahl, Clonal growth of human articular cartilage and the functional role of the periosteum in chondrogenesis, Osteoarthritis Cartilage 13 (2) (2005) 146–153, https://doi.org/10.1016/j.joca.2004.10.020.
[65] I.K. Campbell, U. Novak, J. Cebon, J.E. Layton, J.A. Hamilton, Human articular cartilage and chondrocytes produce hemopoietic colony-stimulating factors in culture in response to IL-1, J. Immunol. 147 (4) (1991) 1238–1246.
[66] N.K. Paschos, W.E. Brown, R. Eswaramoorthy, J.C. Hu, K.A. Athanasiou, Advances in tissue engineering through stem cell-based co-culture, J. Tissue Eng. Regen. Med. 9 (5) (2015) 488–503, https://doi.org/10.1002/term.1870.
[67] E.J. Levorson, M. Santoro, F.K. Kasper, A.G. Mikos, Direct and indirect co-culture of chondrocytes and mesenchymal stem cells for the generation of polymer/extracellular matrix hybrid constructs, Acta Biomater. 10 (5) (2014) 1824–1835, https://doi.org/10.1016/j.actbio.2013.12.026.
[68] J. Fischer, A. Dickhut, M. Rickert, W. Richter, Human articular chondrocytes secrete parathyroid hormone-related protein and inhibit hypertrophy of mesenchymal stem cells in coculture during chondrogenesis, Arthritis Rheum. 62 (9) (2010) 2696–2706, https://doi.org/10.1002/art.27565.
[69] K. Asgarpour, Z. Shojaei, F. Amiri, J. Ai, M. Mahjoubin-Tehran, F. Ghasemi, R. ArefNezhad, M.R. Hamblin, H. Mirzaei, Exosomal microRNAs derived from mesenchymal stem cells: cell-to-cell messages, Cell Commun. Signal. 18 (1) (2020) 149, https://doi.org/10.1186/s12964-020-00650-6.
[70] N.P.T. Huynh, B. Zhang, F. Guilak, High-depth transcriptomic profiling reveals the temporal gene signature of human mesenchymal stem cells during chondrogenesis, FASEB J. 33 (1) (2019) 358–372, https://doi.org/10.1096/fj.201800534R.
[71] L. Xu, Y. Wu, Y. Liu, Y. Zhou, Z. Ye, W.S. Tan, Non-contact coculture reveals a comprehensive response of chondrocytes induced by mesenchymal stem cells through trophic secretion, Tissue Eng. Regen. Med. 15 (1) (2018) 37–48, https://doi.org/10.1007/s13770-017-0084-8.
[72] S. Zhang, P. Hu, T. Liu, Z. Li, Y. Huang, J. Liao, M.R. Hamid, L. Wen, T. Wang, C. Mo, M. Alini, S. Grad, T. Wang, D. Chen, G. Zhou, Kartogenin hydrolysis product 4-aminobiphenyl distributes to cartilage and mediates cartilage regeneration, Theranostics 9 (24) (2019) 7108–7121, https://doi.org/10.7150/thno.38182.
[73] K. Kita, T. Kimura, N. Nakamura, H. Yoshikawa, T. Nakano, PI3K/Akt signaling as a key regulatory pathway for chondrocyte terminal differentiation, Gene Cell. 13 (8) (2008) 839–850, https://doi.org/10.1111/j.1365-2443.2008.01209.x.
[74] H. Qi, D.P. Liu, D.W. Xiao, D.C. Tian, Y.W. Su, S.F. Jin, Exosomes derived from mesenchymal stem cells inhibit mitochondrial dysfunction-induced apoptosis of chondrocytes via p38, ERK, and Akt pathways, in Vitro Cell, Dev. Biol. Anim. 55 (3) (2019) 203–210, https://doi.org/10.1007/s11626-019-00330-x.
[75] B. Sundaram, A.G. Cherian, S. Kumar, 3D decellularized native extracellular matrix scaffold for in vitro culture expansion of human wharton's jelly-derived mesenchymal stem cells (hWJ MSCs), in: K. Turksen (Ed.), Decellularized Scaffolds and Organogenesis: Methods and Protocols, Springer New York, New York, NY, 2018, pp. 35–53.